BJR https://doi.org/10.1259/bjr.20211151

Received: 14 October 2021 | Accepted: 22 June 2022 | Published online: 04 July 2022

Cite this article as:
Huynh AD, Sweet DE, Feldman MK, Remer EM. Imaging of renal emergencies: Review of infectious, hemorrhagic, vascular, and traumatic etiologies. *Br J Radiol* (2022) 10.1259/bjr.20211151.

REVIEW ARTICLE

Imaging of renal emergencies: Review of infectious, hemorrhagic, vascular, and traumatic etiologies

[1]ALAN D. HUYNH, MD, [1]DAVID E. SWEET, MD, [1]MYRA K FELDMAN, MD and [1,2]ERICK M REMER, MD

[1]Imaging Institute, Cleveland Clinic, Cleveland, United States
[2]Glickman Urological and Kidney Institute, Cleveland Clinic, Cleveland, United States

Address correspondence to: Dr Erick M Remer
E-mail: *remere1@ccf.org*

ABSTRACT

Diagnostic imaging allows for accurate and early recognition of acute renal pathologies, thus allowing for appropriate clinical triage, life-saving treatments, and preservation of renal function. In this review, we discuss the clinical presentation and imaging findings of renal emergencies with infectious, hemorrhagic, vascular, and traumatic etiologies.

INTRODUCTION

In patients with emergent renal disorders, prompt initiation of treatment is critical to preserve renal function and reduce morbidity and mortality; however, many of these disorders are characterized by non-specific clinical presentations and unreliable findings on physical examination. Imaging is, therefore, relied upon to establish a diagnosis and direct treatment in a timely manner. Ultrasound (US) is the first-line imaging modality when emergent pathology of a kidney allograft is suspected. When emergencies involving native kidneys are suspected, CT is generally the initial imaging modality of choice, although US can be used when radiation exposure and/or iodinated contrast material is contraindicated (*e.g.,* in pediatric and pregnant patients). More recently, contrast-enhanced ultrasound (CEUS) has become an emerging alternative technique for the detection of select renal vascular disorders (*e.g.,* infarction or cortical necrosis) and for the identification of renal abscesses, but this method is not yet approved for use by the Food and Drug Administration in the United States. Magnetic resonance imaging (MRI) is generally reserved as a problem-solving tool.

In this review, we will examine acute renal pathologies of infectious, hemorrhagic, vascular, and traumatic origins. For each topic, we will review the typical clinical presentation and define key imaging findings used to synthesize a diagnosis, with an emphasis on implications for triage and management.

Infectious etiologies

Urinary tract infections (UTIs) affect up to 150 million people annually worldwide and are a source of substantial morbidity.[1] Most UTIs are treated with antibiotics and require no imaging. In some cases, however, UTIs can become complicated, leading to pyelonephritis, renal or perinephric abscess, pyonephrosis, or emphysematous pyelonephritis/pyelitis. Imaging is indicated when symptoms fail to improve 72 h after initiation of antibiotics or when risk factors are present, including diabetes, immunocompromised state, advanced age, or history of urinary tract obstruction (renal stone disease, congenital or acquired).[2] Intraveneous contrast-enhanced CT (CECT) is the imaging modality of choice for these patients, as it allows for characterization of obstructive uropathy, detection of urolithiasis, and identification of complications including perinephric abscesses and intraparenchymal gas. US may be used when ionizing radiation or iodinated contrast should be avoided or when patients are too sick to travel to the radiology department.[2]

Emphysematous pyelonephritis and emphysematous pyelitis

Emphysematous pyelonephritis is a potentially life-threatening renal parenchymal infection caused by gas-forming bacteria, most often *Escherichia coli* followed by *Klebsiella* species.[3] As with many other complicated UTIs, diabetes and ureteric obstruction are the most common predisposing factors for these infections; more than 90% of cases are associated with diabetes without obstruction.[4] Emphysematous pyelonephritis involves the renal parenchyma and retroperitoneum (Figure 1), whereas emphysematous pyelitis is limited to gas in the collecting system (Figure 2).[4] For emphysematous pyelitis, antibiotic therapy

Figure 1. A 61-year-old female with diabetes was admitted to the intensive care unit with diabetic ketoacidosis and septic shock. (a) Initial scout digital radiograph shows mottled retroperitoneal gas within the right renal fossa (thick arrow) and large pockets of intraperitoneal gas along the right abdominal wall (thin arrows). (b, c) Subsequent axial (b) and coronal (c) contrast-enhanced CT images show near-complete destruction of the right renal parenchyma with extensive intraparenchymal, retroperitoneal, and intraperitoneal gas (arrows), imaging features of emphysematous pyelonephritis.

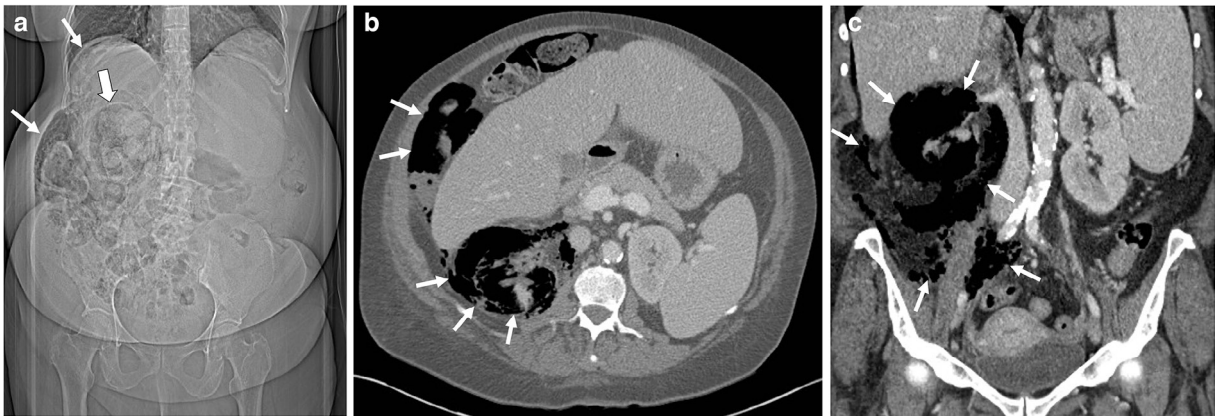

alone is sufficient, with the caveat that removal of any source of obstruction is important. Historically, the treatment of emphysematous pyelonephritis mandated nephrectomy. Contemporary management is guided by the severity and degree of renal involvement, with antibiotic therapy and percutaneous drainage used as the mainstay approaches and surgical intervention used in cases of disease progression or clinical deterioration.[3]

Radiography has a sensitivity as low as 33% for the detection of gas involving the renal parenchyma or perinephric space,[4] which appears as lucency outlining the kidney, and the sensitivity varies depending on the extent, severity, and distribution of gas. Ultrasound in these patients shows linear bright echoes with "dirty" acoustic shadowing, but this modality may be limited in the setting of abundant retroperitoneal gas that obscures the kidney.[4] If clinical suspicion remains high with an indeterminate US examination, CT can be used to confirm and better demonstrate the severity and extent of the disorder, including parenchymal destruction and associated fluid collections, and is more useful for prognostic and treatment guidance. The presence of mottled gas and parenchymal destruction is associated with a higher mortality rate (69%), whereas the presence of bubbly or loculated gas with perirenal fluid collections is associated with a lower mortality rate (18%).[5]

Renal abscess

Renal and perinephric abscesses are localized collections of inflammatory cells that arise as complications from ascending urinary tract infections or, uncommonly, as a result of hematogenous spread. Predisposing factors include the presence of diabetes, nephrolithiasis, and ureteral obstruction. Early diagnosis is critical in these patients, as delayed diagnosis has been correlated with increased mortality.[6] Treatment with intravenous antibiotics and percutaneous drain placement is effective in most patients, but the presence of multiloculated abscesses, emphysematous changes, or underlying diseases (*i.e.,* nephrolithiasis and diabetes) has been associated with antibiotic treatment failure. Refractory cases are treated with nephrectomy, surgical drainage, or percutaneous nephrolithotomy.[6]

For patients with known or suspected renal abscess, US may be used initially, but this modality lacks the accuracy and sensitivity of CT (US accuracy,~75%).[6] On grayscale US images, the involved kidney may appear enlarged, with a focal area or areas of hypoechoic parenchyma demonstrating absent flow on color Doppler US examination. Over time, a distinct wall may be perceptible on grayscale images, with increased vascular flow seen on color Doppler images. Although CEUS is not approved for renal applications in the United States, the European Federation of Societies for Ultrasound in Medicine and Biology (EFSUMB) guidelines suggest that CEUS can be used to assess for complications of pyelopnephritis if the patient remains febrile after 72 h. Renal abscesses contain no internal vascularity, as parenchyma has been destroyed by liquefactive necrosis, and has no central enhancement with CEUS microbubble use.[2,7] CECT demonstrates a low-attenuation collection with an enhancing rim along with other secondary signs of renal infection, including renal enlargement, perinephric stranding, and thickening of Gerota's fascia (Figure 3).[8] MRI demonstrates fluid signal intensity with markedly restricted diffusion.[9]

Pyonephrosis

Pyonephrosis refers to pus in an obstructed and dilated renal collecting system. This condition, which is most often caused by gram-negative bacteria, should be suspected in patients with known urinary tract obstruction who present with fever and flank pain.[8] Imaging helps facilitate early diagnosis and intervention in these patients, preventing the rapid onset of renal failure and sepsis.[10] While sensitivity was historically lower (~62%), this has improved with newer technology.[11] Treatment involves decompressing the collecting system with a percutaneous nephrostomy tube or with placement of a retrograde ureteral internal stent.[12]

Figure 2. A 24-year-old female with diabetes presented with diabetic ketoacidosis and urinary tract infection. (a) Initial sagittal ultrasound image shows an echogenic focus of gas in the left upper pole collecting system with "dirty" shadowing (arrow). (b) Subsequent non-contrast axial CT image shows gas localized in the collecting system without parenchymal involvement (arrows), findings indicating emphysematous pyelitis.

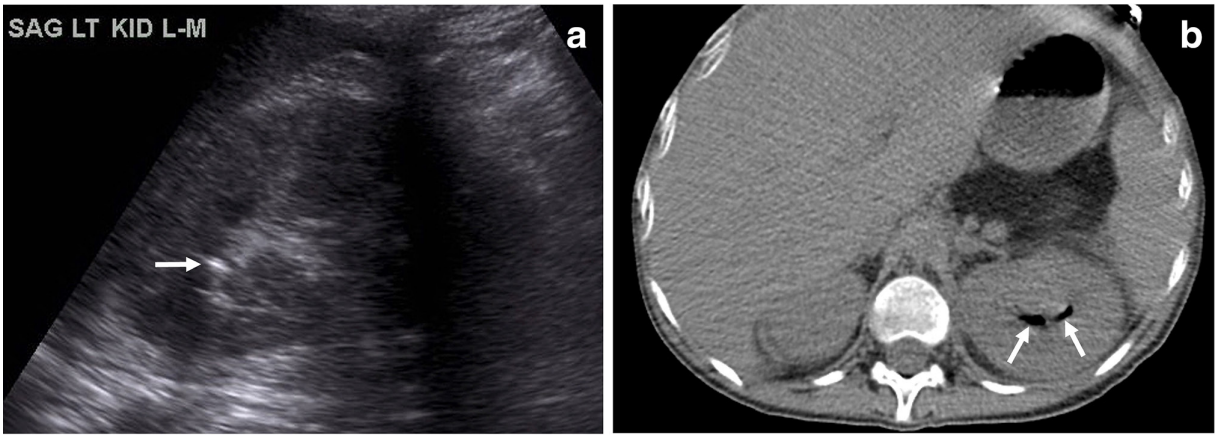

In patients with pyonephrosis, US demonstrates pelvicaliceal dilation, echogenic debris, and fluid-fluid levels within the collecting system with a sensitivity of 90%, a specificity of 97%, and an accuracy of 96% (Figure 4).[10] CECT demonstrates renal pelvic wall thickening (>2 mm), parenchymal or perinephric inflammatory changes, dilation and obstruction of the collecting system with high-attenuation material within the collecting system, and layering of contrast material on excretory images, although more subtle cases may be difficult to distinguish from hydronephrosis. MRI demonstrates findings similar to those seen on CT, including a dilated collecting system with internal debris; on MRI, pyonephrosis can be differentiated from hydronephrosis by the presence of restricted diffusion.[10,13]

Hemorrhagic etiologies

Cases of perinephric renal and retroperitoneal hemorrhage have nonspecific and variable clinical presentations that depend on the amount and duration of hemorrhage. Clinical signs and symptoms may include back and abdominal pain, the presence of a palpable mass, anemia, hypotension, abdominal compartment syndrome, hemodynamic instability, hypovolemic shock, or hypertension secondary to a Page kidney.[14] Retroperitoneal and perinephric hemorrhage can be caused by conditions such as spontaneous hemorrhage (Wunderlich syndrome), trauma, neoplasms, and vascular disorders (*i.e.,* pseudoaneurysm, aneurysm, and arteriovenous malformation [AVM]). (Vascular disorders and trauma are also discussed separately later in this article.) Imaging plays an important role in establishing the diagnosis and determining the underlying cause.

Wunderlich syndrome, defined as spontaneous nontraumatic hemorrhage, can be potentially fatal if not recognized and treated early. It classically presents as Lenk's triad, which consists of flank pain, a palpable tender mass, and hypovolemic shock. Renal neoplasms, particularly angiomyolipomas (AMLs) and renal cell carcinomas (RCCs), are the most common etiologies, with other causative conditions including cystic renal disease, vasculitis, coagulopathy, AVM, aneurysm, inflammatory disease, and urolithiasis.[15] Approximately 5 to 10% of patients with spontaneous renal hemorrhage do not have an identifiable abnormality.[16]

Figure 3. A female receiving immunomodulating therapy for inflammatory bowel disease was admitted with a fever and diagnosed with a urinary tract infection. (a) Sagittal ultrasound (US) image of the right kidney shows diffuse multifocal regions of hypoechogenicity (arrows). (b) Transverse power Doppler US image demonstrates no flow in one of the hypoechoic regions at the mid-pole level (arrows). (c) Coronal contrast-enhanced CT image better delineates multifocal cystic masses/abscesses throughout the right kidney with associated renal swelling. *Klebsiella* infection with multifocal renal abscess was confirmed by aspiration prior to drain placement.

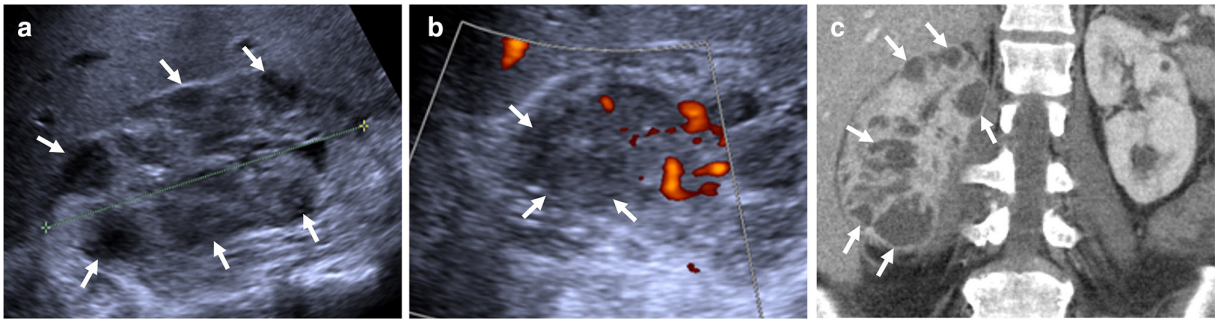

Figure 4. An 86-year-old female with recurrent urinary tract infections presented with fever and septic shock. Sagittal ultrasound image of the right kidney shows echogenic material within a severely dilated collecting system (arrows), which is suggestive of pyonephrosis given the clinical history. Frank pus was noted at the time of a percutaneous nephrostomy catheter placement, confirming the diagnosis of pyonephrosis.

For triage and assessment, US is frequently performed initially as the presentation can be non-specific, although CT is the modality of choice to assess this condition. The sensitivity of US for the detection of perinephric hemorrhage is 76%; US is not effective in determining the source of the bleeding or the underlying pathology.[16] On US, perinephric hematoma appears as a perinephric collection with mass effect on the renal parenchyma that is isoechoic to hyperechoic if acute and hypoechoic to anechoic if subacute or chronic. CT is the preferred initial imaging examination in a nontraumatic setting, allowing identification of the presence, amount, and location of the hemorrhage.[17] On noncontrast CT, acute hemorrhage appears as an area of high attenuation (40–70 HU). On CECT or CT angiography, active contrast extravasation (when present) can be identified as a focal area of high attenuation, similar to blood pool, that persists and becomes larger on delayed images.[15] These techniques can also aid in identifying etiologies such as neoplasm and vascular anomaly. In cases of high clinical suspicion without a definitive diagnosis on CT, CT or MR angiography, or conventional angiography if needed, can be used to assess for vascular etiologies such as polyarteritis nodosa (PAN), aneurysm, or AVM. Conventional angiography also allows for definitive treatment with selective arterial embolization.[16]

On MRI, the appearance of hemorrhage varies since the signal intensity changes as blood products age. Because MRI is infrequently used acutely, subacute and chronic hematomas are most commonly seen. The "concentric ring sign" on MRI is pathognomonic for subacute hematoma, appearing as a thin peripheral rim of low signal intensity on all pulse sequences, corresponding with hemosiderin, and an inner peripheral high T1 signal intensity zone, caused by methemoglobin.[18] Additional findings include a hematocrit effect (fluid-fluid level), especially in the setting of coagulopathy, or very occasionally active contrast extravasation, indicative of active bleeding.[18] If the bleeding source cannot be identified on the initial imaging study, follow-up studies should be performed, as underlying processes could be obscured by hematoma.

The most common cause of spontaneous perirenal hemorrhage is AML, followed closely by RCC. AMLs, which are slow-growing tumors composed of muscle, fat, and blood vessels, are the most common type of benign renal neoplasm. The main complication of AMLs is spontaneous bleeding into the retroperitoneum or renal collecting system (Figure 5). Larger AMLs have a higher incidence of bleeding because of their irregular tortuous vasculature and high frequency of aneurysms. A diameter of 4 cm is considered the traditional cutoff to prompt treatment, although recent research has suggested that other factors should be considered, including patient age and rate of tumor growth.[19] One series suggests that an aneurysm size of 5 mm is a more specific indicator of hemorrhage risk for AMLs.[20] On the other hand, for RCCs, the risk of hemorrhage is independent of size.[16] Clear cell carcinoma is the most common cell type of RCC to cause hemorrhage. Spontaneous renal hemorrhage or rupture may be the first sign of an RCC (Figure 5), and hematoma may conceal the tumor on imaging. In general, for neoplasms leading to hemorrhage, CECT is only moderately sensitive (57%) for demonstrating the underlying neoplasm at the time of presentation.[16] MRI can be used if there is suspicion of an underlying neoplasm that is not well visualized on CT.

Vascular disease, usually in the form of PAN, is the next most common cause of spontaneous renal hemorrhage.[21] PAN is a multisystem necrotizing vasculitis involving small and medium vessels that most commonly involves the renal arteries (80%)

Figure 5. Spontaneous renal hemorrhage in three different patients. (a, b) A male with tuberous sclerosis presented with left flank pain. (a, b) Coronal (a) and axial (b) contrast-enhanced CT images show a large hemorrhagic left renal angiomyolipoma containing macroscopic fat (circles), central high-attenuation active contrast extravasation (thick arrows), and extensive perinephric blood products (thin arrows). A small portion of the left upper pole renal parenchyma is visualized on the coronal image (a, arrowhead). (c, d) A 61-year-old male presented with right flank pain. Axial excretory phase (c) and coronal portal venous phase (d) contrast-enhanced CT images show a newly discovered 8-cm right interpolar renal mass (oval) with poorly visualized margins due to associated spontaneous subcapsular hematoma with adjacent posterior retroperitoneal hemorrhage (arrows). The patient subsequently underwent a right nephrectomy, and pathologic analysis characterized the mass as a papillary renal cell carcinoma. (e, f) A 75-year-old female with chronic atrial fibrillation who was taking warfarin presented with flank pain and weakness. Axial (e) and coronal (f) CECT images show a 15 cm left subcapsular hematoma (arrows). No underlying renal mass is visualized. Laboratory tests demonstrated a supratherapeutic international normalized ratio of 5.6 and a hemoglobin level of 6.9 g dl^{-1}, leading to a diagnosis of anticoagulation-related spontaneous hemorrhage.

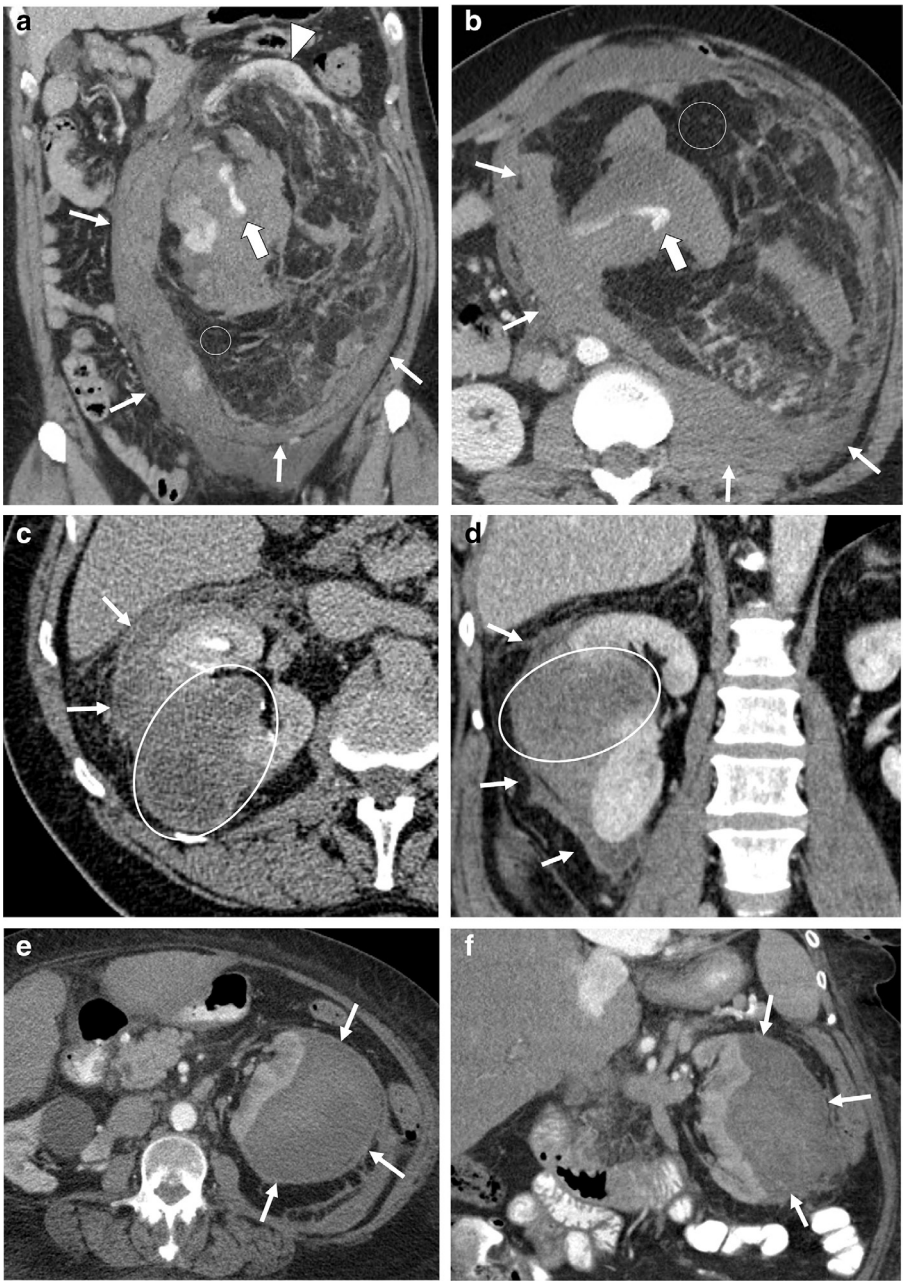

and is thought to be related to autoimmune disease and hepatitis B.[22] Arterial aneurysm rupture can cause spontaneous hemorrhage, which may present unilaterally or bilaterally; PAN should, therefore, be a primary differential consideration in patients with bilateral renal hemorrhage.[16] On CECT, PAN appears as enhancing arterial microaneurysms. In some patients, these

microaneurysms may thrombose, leading to distal hypoperfusion and renal infarction. On angiography, aneurysms of varying sizes can be seen, with the presence of multiple small aneurysms nearly 100% specific for PAN.[22] Treatment for these patients involves angioembolization.

Anticoagulation-related spontaneous retroperitoneal hemorrhage, another cause of spontaneous renal hemorrhage, is associated with a mortality rate as high as 19% within 6 months.[23] Because of the nonspecific symptoms of this condition, 10% of cases are misdiagnosed upon initial encounter. Supratherapeutic anticoagulation and polypharmacy are risk factors for major bleeding, especially in the elderly population. Patients with this condition are treated with coagulopathy reversal, reversal of anticoagulation, and blood products as needed. Invasive approaches are reserved for patients who are refractory to conservative treatment and for patients with mass effect or compressive symptoms.[23] Findings on CT typically include a nonhomogeneous retroperitoneal hyperdense mass (60–80 HU) with a dependent hyperdense component (Figure 5).[24]

Vascular etiologies

Vascular emergencies may be caused by underlying vascular pathologies or by compromise of the renal vasculature. CECT is often the initial imaging modality of choice for underlying processes in native kidneys, but US is preferred for evaluating kidney allografts.

Renal pseudoaneurysm

Renal pseudoaneurysms are arterial wall disruptions that allow constrained hemorrhage into the adjacent renal parenchyma or capsule. They may occur after trauma (including biopsy) or after surgical interventions (*e.g.,* partial nephrectomy), and they may occur at arterial anastomoses or within the renal parenchyma. Patients may be asymptomatic or may present with nonspecific symptoms and signs such as gross hematuria, bleeding, pain, and decreased renal function.[25] Renal pseudoaneurysms can be managed surgically or with minimally invasive radiologic treatments, including percutaneous management, or endoluminal management. Treatment is recommended for symptomatic patients (intermittent or continuous bleeding), or for asymptomatic pseudoaneruysms that enlarge, do not resolve, or become symptomatic.[26] Unstable or active bleeding cases require urgent intervention.[25]

On grayscale US images, pseudoaneurysms appear as anechoic cystic structures adjacent to blood vessels. A neck connecting the pseudoaneurysm to the feeding artery may be identified on grayscale or color Doppler US images. Color Doppler images typically show a "yin-yang" pattern of flow, with a to-and-fro pattern seen on spectral Doppler images. On unenhanced CT, the pseudoaneurysm appears as a low-attenuation rounded structure arising at an arterial anastomosis or within the renal parenchyma that may partially enhance on CECT depending on the degree of thrombosis.[26] MR angiography demonstrates similar findings and can also be used to assess the pseudoaneurysm sac size and degree of intraluminal thrombus, although this evaluation may be limited by artifacts from motion, pulsatility, turbulent flow, and metallic clips or hardware.[26,27] Conventinoal angiography is typically reserved for cases with unclear anatomy and for those requiring endovascular treatment (Figure 6).[27]

Renal Artery Aneurysm

A renal artery aneurysm (RAA) is defined as dilation of the renal artery with preservation of all three layers of the arterial wall. These aneurysms affect an estimated 0.09% of the population and are increasingly encountered incidentally because of the expanding use of cross-sectional imaging.[28] The most common causes include fibromuscular dysplasia, vessel degeneration, vasculitis, and trauma. Traditionally, treatment is suggested for RAAs > 2 cm, for patients with symptoms, and for females of childbearing age (because of the high mortality associated with aneurysm rupture during pregnancy).[28] More recent research, however, has proposed a size cutoff >3 cm and rapid growth as criteria for treatment.[28] Treatment options for RAAs include

Figure 6. A patient presented with flank pain after undergoing a left partial nephrectomy for renal cell carcinoma. (a) Axial contrast-enhanced CT image shows a rounded hyperenhancing pseudoaneurysm at the site of the partial nephrectomy in the left interpolar region (thick arrow), with a surrounding perinephric hematoma containing gas related to the surgical hemostatic agent (arrows). (b) Subsequent digital subtraction angiography image of the left kidney demonstrates three well-defined saccular outpouchings off the renal interlobar arteries, which are pseudoaneurysms.

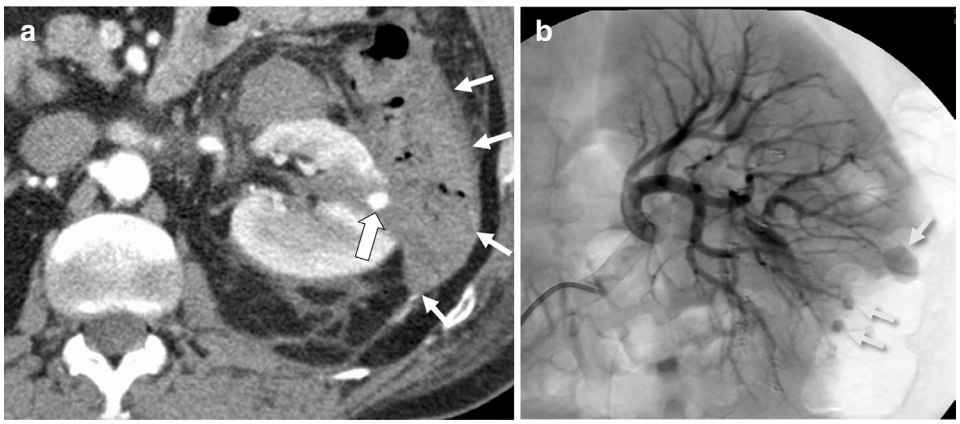

open aneurysm repair or endovascular repair with stent placement and coil embolization.[28]

US allows characterization of the size and location of RAAs. On grayscale US images, an RAA appears as dilation of the renal artery, with flow seen on Doppler images. For RAAs, CT angiography provides higher reproducibility and better anatomic detail of the renal vasculature with less operator dependence compared to US. On CT, an RAA appears as saccular, non-calcified artery dilation, most commonly at the bifurcation of the main renal artery.[29] Conventional angiography is used for endovascular treatment.[27]

Renal AVM

Renal AVMs, which are abnormal communications between arteries and veins outside the capillary level, present with hematuria in 75% of patients.[30] This hematuria is caused by dysplastic vessel rupture within the collecting system and may become life threatening in cases of major blood loss. The severity of hematuria is not correlated to the size of the AVM, as even small renal AVMs may lead to severe blood loss if they are located near the pelvicalyceal system.[30] Asymptomatic small peripheral AVMs without hemodynamic effects can be managed conservatively, but AVMs manifesting with hematuria require urgent treatment. Transcatheter arterial embolization has become the management of choice.[30] Total or partial nephrectomy is reserved for patients in whom embolization has failed.

AVMs appear as hypoechoic cystic or tubular structures on grayscale US images, with color Doppler demonstrating multidirectional flow and aliasing from high flow velocities. Spectral Doppler imaging shows high-velocity, turbulent flow with low-resistance waveforms. CT and MRI demonstrate hyperenhancing foci on contrast examinations, with variable appearance of dilated draining veins and filling of the IVC. Smaller AVMs may be detected only with digital subtraction angiography.[30]

Vascular compromise

Renal infarcts result from blockage of arterial or venous flow and typically present clinically as acute flank pain; however, unanticipated infarcts are often found during routine CT. Bland or septic thromboembolism are the most common causes of renal infarcts; other etiologies include renal vein thrombosis, trauma, dissection, vasculitis, and hypercoagulability. Renal infarct may be suspected on US, but the appearance on grayscale images varies widely, ranging from a normal appearance in the acute setting to a hypoechoic or echogenic mass during later stages. Doppler US imaging demonstrates absence of blood flow with global or major segmental infarction.[31] CECT is the imaging modality of choice for patients with known or suspected renal infarcts. On CECT, the infarct appearance varies based on its degree, location, etiology, and age. Smaller focal infarcts appear as wedge-shaped low-attenuation areas with an apex toward the renal sinus. Larger and global infarcts may affect the entire kidney and may be associated with mass effect and the "cortical rim sign."[32] This sign describes a thin enhancing viable rim of subcapsular cortex that is caused by perforating collateral vessels perfusing the outer rim of the renal cortex in the presence of main renal artery occlusion (Figure 7).[33] "Flip-flop enhancement," a pattern of eventual enhancement in initially hypodense infarcts on delayed phase imaging may also be seen.[32] For patients with renal impairment for whom CECT is no longer preferred, CEUS has been shown to be of comparable accuracy to CT in diagnosing renal infarction, and is significantly more accurate than grayscale and Doppler US alone. CEUS has the added benefit of being able to differentiate between non-perfused, infarcted tissue and hypoperfused parenchymal regions. On CEUS, focal infarcts appear as wedge-shaped non-enhancing areas within an otherwise enhanced kidney.[7] On MRI, there is loss of corticomedullary differentiation, low signal intensity on T_1-weighted and T_2-weighted images, poor enhancement of the affected region, and associated restricted diffusion.[34,35] After the acute phase, renal atrophy corresponding to the severity of the infarct is seen.[32]

Acute cortical necrosis is a rare cause of acute renal failure. This condition is caused by a substantial reduction of renal blood flow with relative sparing of the renal medulla, with most cases affecting both kidneys. Acute cortical necrosis may result from any condition of severe and prolonged shock, including hypovolemia, sepsis, transfusion reaction, and dehydration. Patients present clinically with protracted severe oliguria or anuria. Early diagnosis and visualization of the extent of cortical necrosis allow for prognostic evaluation and treatment planning, including early arrangements for dialysis. Findings for this condition on US are non-specific. CT demonstrates diagnostic findings of abrupt termination of contrast material in the renal artery ("arterial cutoff sign") on arterial phase images, enhancement of the renal medulla with hypoattenuating cortex ("reverse rim sign") on parenchymal phase images, and absent contrast excretion on delayed phase images (Figure 8).[36,37] CEUS can be used to confidently differentiate between acute cortical necrosis and renal infarction. The reverse rim sign appears similar on CEUS and appears as hypoechoic non-enhancing renal cortex with adjacent normal enhancing renal medulla.[38]

Renal transplantation

An increasing number of patients are living with kidney allografts. For these patients, imaging plays an important role in identifying postoperative complications and allograft dysfunction and failure, allowing for treatment planning. Ultrasound is the first-line imaging modality for suspected vascular complications of renal transplantation, especially in the early postoperative period.

Transplant renal artery stenosis is the most common vascular complication, with a prevalence of up to 10%.[39] This condition is a major cause of graft loss and premature death. Most cases occur within the first 6 months after transplantation, with patients often presenting with new-onset hypertension or graft dysfunction.[39] The stenosis most commonly occurs within 1 to 2 cm of the arterial anastomosis. Prompt diagnosis and treatment of this condition, typically with angioplasty with possible stent placement, can prevent allograft damage and systemic sequelae. Color Doppler US imaging shows narrowing of the vessel lumen with focal aliasing. Spectral Doppler imaging shows a 2.5-fold velocity gradient between the stenotic and poststenotic segments, with

Figure 7. A patient with atrial fibrillation presented with new-onset flank pain. (a, b) Coronal (a) and axial (b) contrast-enhanced CT (CECT) images show a wedge-shaped region of nonenhancing renal parenchyma in the left interpolar region. The apex of the wedge-shaped abnormality is directed toward the renal sinus (arrowheads), and there is preserved capsular enhancement overlying the base (cortical rim sign) (arrows). These findings indicate a segmental renal infarct of the left interpolar region. (c, d) Subsequent coronal (c) and axial (d) CECT images performed several years later show expected changes of chronic infarction, with capsular retraction and parenchyma atrophy in the region of the infarction (arrows).

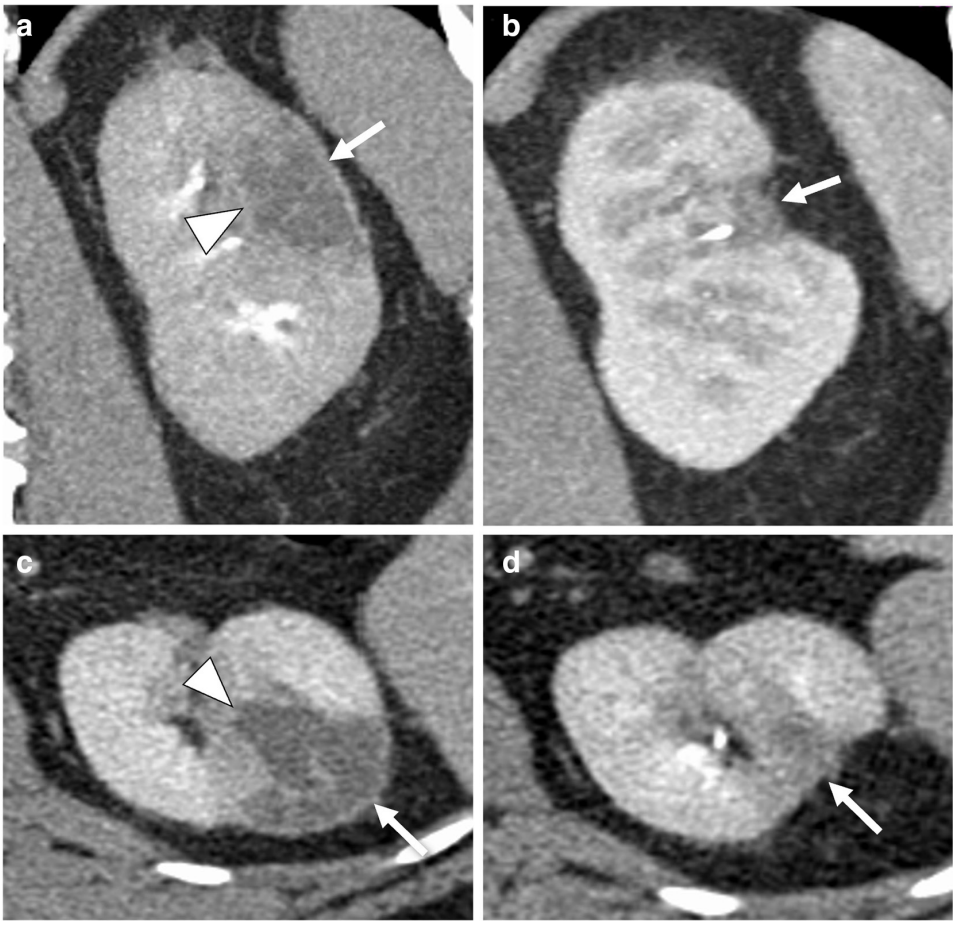

poststenotic spectral broadening. Peak systolic velocities are often elevated to at least 250 to 300 cm/s. Intrarenal arteries may show tardus parvus waveforms, which have a delayed systolic upstroke (acceleration time >0.07 s), a low systolic peak with rounded appearance, and a low resistive index (<0.5) (Figure 9).[39] When US is non-diagnostic or inconclusive, MR angiography and CT angiography can show arterial narrowing.

Transplant renal artery thrombosis occurs in less than 1% of patients, typically in the immediate postoperative period, with a

Figure 8. Images from a 62-year-old male with oliguria and septic shock requiring vasopressor support. (a, b) Coronal (a) and axial (b) contrast-enhanced CT images show diffuse bilateral renal cortical low-attenuation areas (thin arrows), which is diagnostic of acute cortical necrosis. An unrelated nonobstructing right interpolar calculus is present (thick arrow).

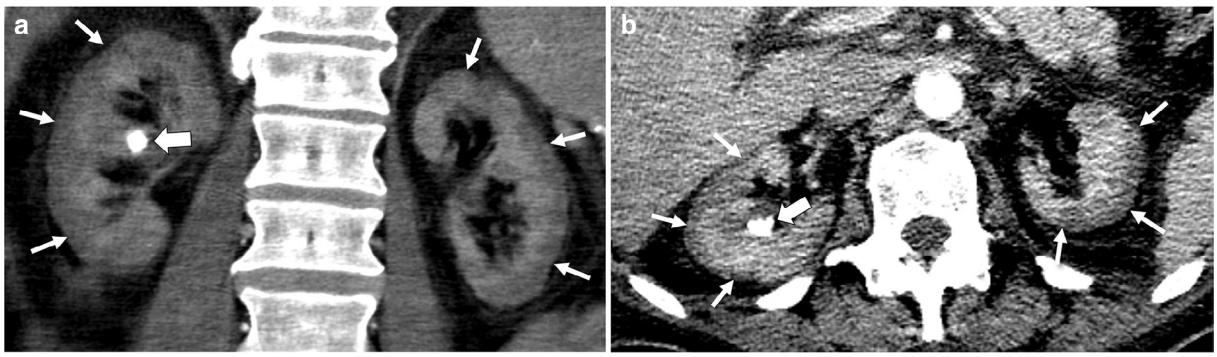

Figure 9. A patient presented with an elevated creatinine level 3 months after undergoing a kidney transplant. (a, b) Color (a) and spectral (b) Doppler ultrasound images of the kidney allograft show focal aliasing at the main renal artery anastomosis (a, circle) with elevated peak systolic velocity of 580 cm/s. A 3.5-fold velocity gradient was present relative to the immediate downstream (poststenotic) mid renal artery (not shown). (c, d) Spectral waveforms of interpolar (c) and lower pole (d) arcuate arteries show a tardus parvus waveform with delayed upstroke, rounded systolic peak, and increased diastolic flow, indicating transplant renal artery stenosis.

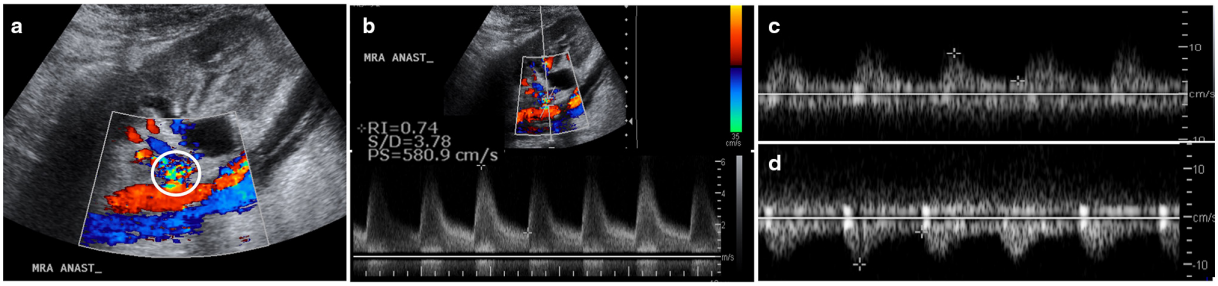

peak incidence at 48 h.[39] Early thrombosis (<14 d) is usually due to surgical technical errors and rarely caused by acute tubular necrosis or allograft rejection, whereas late thrombosis (>14 d) is almost always related to trauma. Patients typically present with sudden anuria, graft tenderness, pain, and thrombocytopenia. This condition may be treated with surgical revascularization or catheter-directed thrombolysis.[39] Doppler images in these patients show no flow within the renal parenchyma or transplanted renal artery. Power Doppler imaging has a higher sensitivity than color Doppler imaging to depict slow blood flow and may be used to distinguish between absent and slow flow (Figure 10).[39] Graft-saving interventions are time sensitive; thus, confirmatory imaging after US is typically not performed.

Transplant renal vein thrombosis occurs in up to 3 to 4% of patients undergoing kidney transplantation, usually within the first 2 weeks after surgery.[39] Thrombosis often results in graft failure, but early detection and treatment with emergent exploratory surgery with thrombectomy and revascularization may salvage some grafts.[39] US shows absent flow within the renal vein on color and spectral Doppler imaging, and the intraparenchymal renal arteries show high-resistance waveforms, sometimes with reversal of diastolic flow (Figure 11).

Renal transplant vascular torsion is a rare complication caused by rotation of the allograft around the renal vascular pedicle. This condition requires prompt diagnosis and surgery to salvage function. Torsion occurs less frequently in extraperitoneal allografts than in those with intraperitoneal placement, likely because of decreased mobility in the extraperitoneal space. The finding most suggestive for this complication is change in axis of the allograft in comparison with previous studies. In affected patients, ureteral compromise causes renal allograft hydronephrosis and edematous enlargement. On spectral Doppler imaging, early or incomplete torsion demonstrates venous compromise with an elevated renal artery resistive index and an elevated velocity at the main renal artery anastomosis, with possible progression to reversed diastolic flow (Figure 12). Complete torsion may result in arterial compromise with decreased resistive index and complete lack of blood flow on color Doppler imaging.[39]

Traumatic etiologies

The kidneys are damaged in up to 3% of patients experiencing trauma, usually in the setting of blunt trauma.[40] Hematuria is the most common clinical presentation, but absence of hematuria does not preclude substantial renal injury. The American Urological Association guidelines state that CECT should be performed in all hemodynamically stable patients who have experienced blunt

Figure 10. A 39-year-old female presented with anuria 1day after undergoing a right iliac fossa kidney transplant. (a) Sagittal power Doppler ultrasound image shows no detectable flow in the kidney allograft. (b, c) Subsequent ^{99m}Tc–labelled mercaptoacetyltriglycine scan shows no flow on the vascular phase in the expected location of the kidney allograft (oval) and is photopenic on more delayed-phase images (oval), which is highly consistent with renal artery thrombosis.

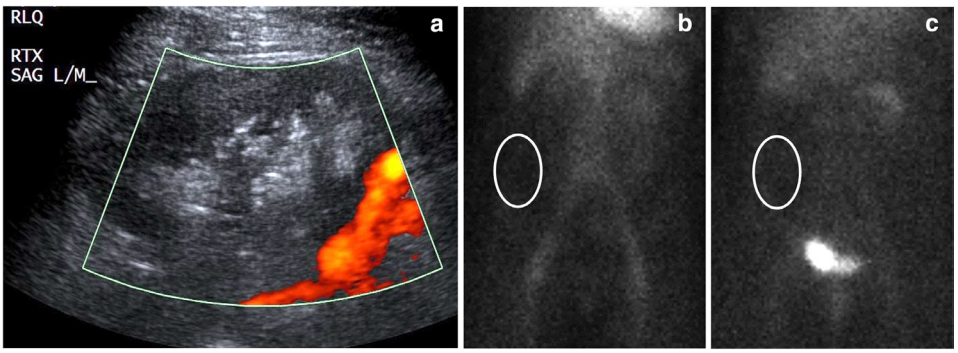

Figure 11. A 52-year-old male presented with an elevated creatinine level 1 day after undergoing a right iliac fossa kidney transplant. (a, b) Transverse color Doppler US images of the kidney allograft centered at the renal vein hilum (a) and mid area (b) show no flow in the main renal vein (arrows). (c-e) Spectral Doppler US images of the transplanted renal artery (c), inferior arcuate artery (d), and mid arcuate artery (e) show arterial resistive indices of 1.0 with diastolic flow reversal throughout the transplanted renal arteries (arrows), further supporting the diagnosis of transplant renal vein thrombosis.

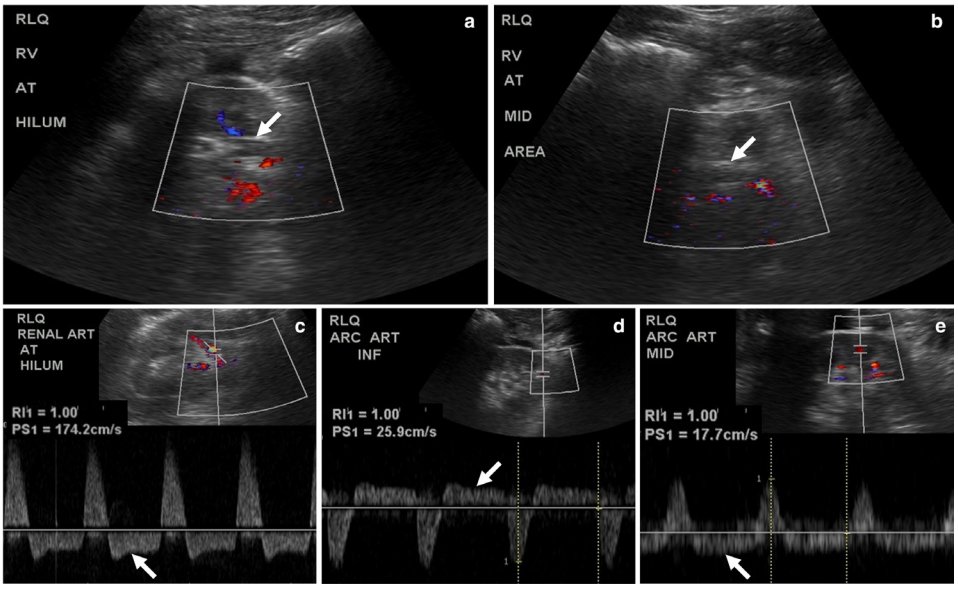

trauma and have either gross hematuria or microscopic hematuria and hypotension, as CT can be used to differentiate between injuries that can be monitored expectantly and those that require intervention. Precontrast, postcontrast arterial, nephrographic, and delayed phases should be obtained. Non-contrast CT can be used to identify calculi and parenchymal hematoma, whereas postcontrast phases can be used to identify parenchymal and vascular damage, intravascular or collecting system contrast extravasation, and other solid organ damage.[40] Hemodynamically unstable patients should first be assessed with a US Focused Assessment with Sonography in Trauma (FAST) examination to identify the presence of free fluid, lacerations, and hematomas; however, compared with CECT, US has poorer

Figure 12. A patient presented with an elevated creatinine level a few days after undergoing a kidney transplant. (a-c) Baseline postoperative images show a normal-appearing kidney allograft, including a sagittal grayscale ultrasound (US) image (a), color and spectral Doppler US image (b) of the transplanted renal artery demonstrating a peak systolic velocity of 117 cm/s and resistive index of 0.82 (within the expected range), and axial noncontrast CT image (c) showing the allograft hilum in a slightly right posterolateral orientation (oval). Repeat imaging was performed after an elevated creatinine level was detected. (d) sagittal US image shows substantial graft enlargement and new moderate hydronephrosis (arrows). (e) Color and spectral Doppler US image of the transplanted renal artery demonstrates decreased diastolic flow, resulting in increased resistive index (arrows). (f)Axial non-contrast CT image again demonstrates hydronephrosis (arrow) and an associated change in graft axis, with the hilum now oriented in an anterolateral direction (oval), indicating renal transplant torsion. The patient underwent immediate surgical detorsion. Case courtesy of Mindy M. Horrow, MD, Einstein Medical Center, Philadelphia, Pennsylvania.

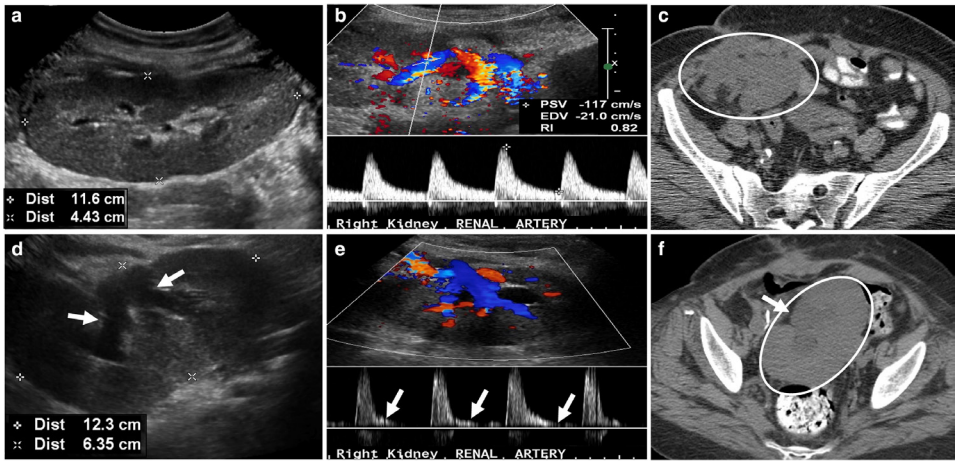

Figure 13. Increasing severity of traumatic renal injury in 4 patients. (a, b) Grade 1 kidney injury from a fall off a ladder. Axial (a) and coronal (b) CECT images of the left kidney show a focal area of decreased renal parenchymal enhancement (thin arrow) relative to normal adjacent regions (arrows) representing a renal contusion with an associated left crescentic subcapsular hematoma (thick arrows), consistent with Grade 1 kidney injury. (c, d) Grade 3 kidney injury from a motor vehicle collision. (c) Axial nephrographic Phase CECT image demonstrates a cortical laceration greater than 1 cm in depth with extension to the renal pelvis (arrowhead) and associated moderate-sized perinephric hematoma (thin arrows). (d) Delayed coronal excretory Phase CECT image shows that the collecting system is intact without urinary contrast extravasation (thick arrows). (e, f) Grade 4 kidney injury in a different patient. (e) Axial CECT nephrographic Phase image shows layering high-attenuation hematoma in the right renal pelvis (thin arrows) with perinephric low-attenuation fluid (thick arrows). (f) Subsequent axial CECT delayed phase image confirms a right collecting system injury with excreted contrast spillage into the perinephric space (thick arrows), indicating a Grade four kidney injury. (g-i) Grade 5 kidney injury from a bicycle collision. (g) Sagittal CECT image of the left kidney shows extensive renal parenchymal and perirenal hemorrhage (thin arrows) with foci of active contrast extravasation in the region of the upper pole (thick arrow). (h) Left renal arteriogram confirms active bleeding from an upper pole renal artery branch (arrows). (i) Subsequent digital subtraction left renal arteriogram obtained after coil embolization demonstrates resolution of the bleeding (arrowhead). Cases of Grades 4 and 5 kidney injury (images e-i) are courtesy of David D. Casalino, MD, Northwestern Memorial Hospital, Chicago, Illinois.

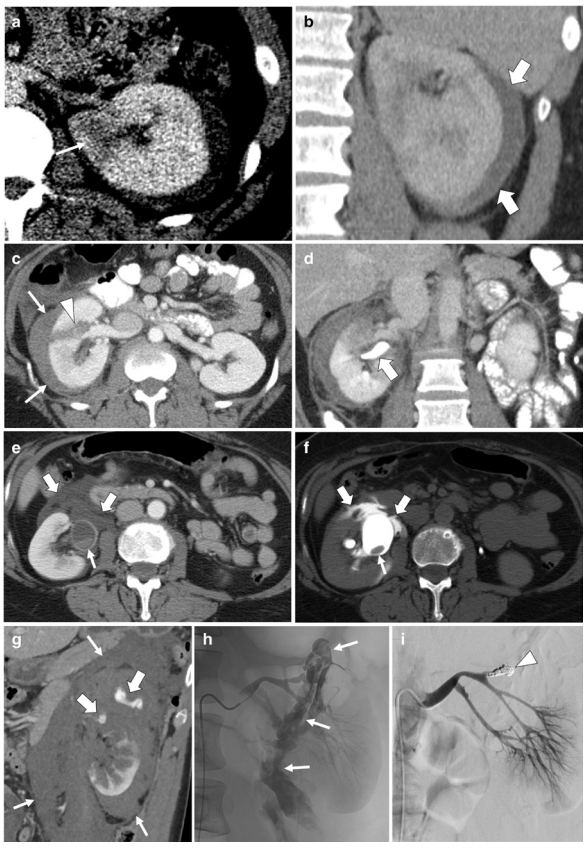

sensitivity for retroperitoneal hemorrhage and minor renal injuries, inferior resolution, inability to distinguish fresh blood from extravasated urine, and inability to identify vascular pedicle injuries and segmental infarct.[40,41]

The commonly used American Association for the Surgery of Trauma (AAST) renal trauma classification system describes the severity of renal injury on a scale from 1 to 5 based on the degree of parenchymal damage and vascular and collecting system involvement.[40] Grade 1 and 2 injuries are generally managed conservatively with observation and supportive care, with reimaging performed in cases of patient deterioration. Grade 1 renal injuries (22%–28% of cases) present with microscopic or gross hematuria with normal imaging, a renal contusion, or a non-expanding subcapsular hematoma without parenchymal laceration. Renal contusion appears as a focal area of decreased parenchymal enhancement and may have sharply or poorly defined margins. Small subcapsular hematomas appear as crescentic hyperattenuation (40–60 HU) adjacent to the parenchyma with minimal mass effect; if large, the hematoma can assume a biconvex appearance (Figure 13). Grade 2 injuries (28%–30% of cases) appear as nonexpanding perirenal hematomas confined to the retroperitoneum with or without a superficial laceration (<1 cm in depth) in the renal cortex.[40]

Grade 3 injuries (20%–26% of cases) include deep lacerations (>1 cm in depth) with vascular injury (defined as pseudoaneurysm or arteriovenous fistula) or active bleeding contained within Gerota's fascia and without extension into the collecting system or urinary extravasation (Figure 13). Grade four injuries (15%–19% of cases) include lacerations extending through the renal cortex, medulla, and collecting systems; injuries to the renal vasculature with hemorrhage beyond Gerota's fascia; vascular injuries, including thrombosis, segmental renal artery or vein injuries; and all collecting system injuries.[40,42] Treatment for Grades 3 and 4 injuries depends on the extent of injury and may include angioembolization for bleeding, ureteral stent insertion for collecting system leaks, and sometimes delayed surgery.[40] Of note, urinary extravasation in Grade 4 injuries will resolve spontaneously in up to 87% of patients, so collecting system injury alone (as detected on excretory phase imaging) is not an indication for surgery.[43] On CT, lacerations in patients with Grade 3 or four injuries appear as low-attenuation linear areas in the parenchyma that can be associated with hemorrhage. Active hemorrhage, which appears as extravasation of contrast medium (measuring within 10–15 HU of blood pool contrast) surrounded by lower attenuation clotted blood, is an important indicator of impending decompensation. Urinary extravasation appears as contrast material surrounding the kidney during the pyelographic or delayed phases.[44] Infarction occurs with segmental arterial thrombosis or laceration and appears as peripheral wedge-shaped parenchymal hypoattenuation.

Grade 5 injuries (6%–7% of cases) consist of lacerations that completely shatter the kidney, injuries to the renal hilum with devascularization of the kidney and active bleeding, traumatic renal arterial disruption, and traumatic renal artery occlusion (Figure 13).[40,42] Complete devascularization may occur with or without parenchymal lacerations, and extensive retroperitoneal hemorrhage and hematuria may be absent in cases of isolated intimal injury to the renal artery resulting in thrombosis. For hemodynamically unstable patients with

actively bleeding renovascular pedicle injuries, surgical exploration is indicated to prevent exsanguination. Renal artery thrombosis or avulsion should be treated rapidly to prevent permanent progressive loss of renal function, with most authors agreeing that repair must occur within 4h of injury to preserve meaningful renal function.[44] On CT, traumatic renal infarction appears as an abrupt truncation of the artery, an absent renal nephrogram, and retrograde opacification of the renal vein from the IVC.[44]

CONCLUSION

Renal emergencies encompass a wide variety of pathologies that include **infectious, hemorrhagic, vascular, and traumatic causes**. Many may manifest with non-specific clinical presentations. Imaging examinations allow clinicians to rapidly diagnose these different pathologies, equipping the clinical team with the information needed for appropriate treatment planning.

ACKNOWLEDGEMENTS

The authors would like to acknowledge Megan Griffiths for her expert editing assistance.

REFERENCES

1. Flores-Mireles AL, Walker JN, Caparon M, Hultgren SJ. Urinary tract infections: epidemiology, mechanisms of infection and treatment options. *Nat Rev Microbiol* 2015; **13**: 269–84. https://doi.org/10.1038/nrmicro3432
2. Nikolaidis P, Dogra VS, Goldfarb S, Gore JL, Harvin HJ, Heilbrun ME, et al. ACR appropriateness criteria® acute pyelonephritis. *Journal of the American College of Radiology* 2018; **15**: S232–39. https://doi.org/10.1016/j.jacr.2018.09.011
3. Aswathaman K, Gopalakrishnan G, Gnanaraj L, Chacko NK, Kekre NS, Devasia A. Emphysematous pyelonephritis: outcome of conservative management. *Urology* 2008; **71**: 1007–9. https://doi.org/10.1016/j.urology.2007.12.095
4. Tsitouridis I, Michaelides M, Sidiropoulos D, Arvanity M. Renal emphysema in diabetic patients: CT evaluation. *Diagn Interv Radiol* 2010; **16**: 221–26. https://doi.org/10.4261/1305-3825.DIR.2130-08.1
5. Wan YL, Lee TY, Bullard MJ, Tsai CC. Acute gas-producing bacterial renal infection: correlation between imaging findings and clinical outcome. *Radiology* 1996; **198**: 433–38. https://doi.org/10.1148/radiology.198.2.8596845
6. Yen DH, Hu SC, Tsai J, Kao WF, Chern CH, Wang LM, et al. Renal abscess: early diagnosis and treatment. *Am J Emerg Med* 1999; **17**: 192–97. https://doi.org/10.1016/s0735-6757(99)90060-8
7. Piscaglia F, Nolsøe C, Dietrich CF, Cosgrove DO, Gilja OH, Bachmann Nielsen M, et al. The EFSUMB guidelines and recommendations on the clinical practice of contrast enhanced ultrasound (CEUS): update 2011 on non-hepatic applications. *Ultraschall Med* 2012; **33**: 33–59. https://doi.org/10.1055/s-0031-1281676
8. Vourganti S, Agarwal PK, Bodner DR, Dogra VS. Ultrasonographic evaluation of renal infections. *Radiol Clin North Am* 2006; **44**: 763–75. https://doi.org/10.1016/j.rcl.2006.10.001
9. Goyal A, Sharma R, Bhalla AS, Gamanagatti S, Seth A. Diffusion-weighted MRI in inflammatory renal lesions: all that glitters is not RCC! *Eur Radiol* 2013; **23**: 272–79. https://doi.org/10.1007/s00330-012-2577-0
10. Craig WD, Wagner BJ, Travis MD. Pyelonephritis: radiologic-pathologic review. *Radiographics* 2008; **28**: 255–77; . https://doi.org/10.1148/rg.281075171
11. Jeffrey RB, Laing FC, Wing VW, Hoddick W. Sensitivity of sonography in pyonephrosis: a reevaluation. *AJR Am J Roentgenol* 1985; **144**: 71–73. https://doi.org/10.2214/ajr.144.1.71
12. Li AC, Regalado SP. Emergent percutaneous nephrostomy for the diagnosis and management of pyonephrosis. *Semin Intervent Radiol* 2012; **29**: 218–25. https://doi.org/10.1055/s-0032-1326932
13. Chan JH, Tsui EY, Luk SH, Fung SL, Cheung YK, Chan MS, et al. MR diffusion-weighted imaging of kidney: differentiation between hydronephrosis and pyonephrosis. *Clin Imaging* 2001; **25**: 110–13. https://doi.org/10.1016/s0899-7071(01)00246-7
14. Vijayganapathy S, Karthikeyan VS, Mallya A, Sreenivas J. Page kidney in wunderlich syndrome causing acute renal failure and urosepsis: successful timely minimally invasive management of a devastating clinical entity. *J Clin Diagn Res* 2017; **11**: PD03–4. https://doi.org/10.7860/JCDR/2017/24731.9963
15. Katabathina VS, Katre R, Prasad SR, Surabhi VR, Shanbhogue AKP, Sunnapwar A. Wunderlich syndrome: cross-sectional imaging review. *J Comput Assist Tomogr* 2011; **35**: 425–33. https://doi.org/10.1097/RCT.0b013e3182203c5e
16. Zhang JQ, Fielding JR, Zou KH. Etiology of spontaneous perirenal hemorrhage: a meta-analysis. *J Urol* 2002; **167**: 1593–96. https://doi.org/10.1097/00005392-200204000-00006
17. Katz DS, Lane MJ, Mindelzun RE. Unenhanced CT of abdominal and pelvic hemorrhage. *Semin Ultrasound CT MR* 1999; **20**: 94–107. https://doi.org/10.1016/s0887-2171(99)90041-0
18. Goenka AH, Shah SN, Remer EM. Imaging of the retroperitoneum. *Radiol Clin North Am* 2012; **50**: 333–55, . https://doi.org/10.1016/j.rcl.2012.02.004
19. Fernández-Pello S, Hora M, Kuusk T, Tahbaz R, Dabestani S, Abu-Ghanem Y, et al. Management of sporadic renal angiomyolipomas: a systematic review of available evidence to guide recommendations from the european association of urology renal cell carcinoma guidelines panel. *Eur Urol Oncol* 2020; **3**: 57–72. https://doi.org/10.1016/j.euo.2019.04.005
20. Yamakado K, Tanaka N, Nakagawa T, Kobayashi S, Yanagawa M, Takeda K. Renal angiomyolipoma: relationships between tumor size, aneurysm formation, and rupture. *Radiology* 2002; **225**: 78–82. https://doi.org/10.1148/radiol.2251011477
21. Ahn T, Roberts MJ, Navaratnam A, Chung E, Wood S. Changing etiology and management patterns for spontaneous renal hemorrhage: a systematic review of contemporary series. *Int Urol Nephrol* 2017; **49**: 1897–1905. https://doi.org/10.1007/s11255-017-1694-8
22. Allen AW, Waybill PN, Singh H, Brown DB. Polyarteritis nodosa presenting as spontaneous perirenal hemorrhage: angiographic diagnosis and treatment with microcoil embolization. *J Vasc Interv Radiol* 1999; **10**: 1361–63. https://doi.org/10.1016/s1051-0443(99)70244-7
23. Sunga KL, Bellolio MF, Gilmore RM, Cabrera D. Spontaneous retroperitoneal hematoma: etiology, characteristics, management, and outcome. *J Emerg Med* 2012; **43**: e157-61.

https://doi.org/10.1016/j.jemermed.2011.06.006
24. Zissin R, Ellis M, Gayer G. The CT findings of abdominal anticoagulant-related hematomas. *Semin Ultrasound CT MR* 2006; **27**: 117–25. https://doi.org/10.1053/j.sult.2006.01.008
25. Ghoneim TP, Thornton RH, Solomon SB, Adamy A, Favaretto RL, Russo P. Selective arterial embolization for pseudoaneurysms and arteriovenous fistula of renal artery branches following partial nephrectomy. *J Urol* 2011; **185**: 2061–65. https://doi.org/10.1016/j.juro.2011.02.049
26. Saad NEA, Saad WEA, Davies MG, Waldman DL, Fultz PJ, Rubens DJ. Pseudoaneurysms and the role of minimally invasive techniques in their management. *Radiographics* 2005; **25 Suppl 1**: S173-89. https://doi.org/10.1148/rg.25si055503
27. Cura M, Elmerhi F, Bugnogne A, Palacios R, Suri R, Dalsaso T. Renal aneurysms and pseudoaneurysms. *Clin Imaging* 2011; **35**: 29–41. https://doi.org/10.1016/j.clinimag.2009.12.001
28. Klausner JQ, Lawrence PF, Harlander-Locke MP, Coleman DM, Stanley JC, Fujimura N, et al. The contemporary management of renal artery aneurysms. *J Vasc Surg* 2015; **61**: 978–84. https://doi.org/10.1016/j.jvs.2014.10.107
29. Nosher JL, Chung J, Brevetti LS, Graham AM, Siegel RL. Visceral and renal artery aneurysms: a pictorial essay on endovascular therapy. *Radiographics* 2006; **26**: 1687–1704; . https://doi.org/10.1148/rg.266055732
30. Hatzidakis A, Rossi M, Mamoulakis C, Kehagias E, Orgera G, Krokidis M, et al. Management of renal arteriovenous malformations: A pictorial review. *Insights Imaging* 2014; **5**: 523–30. https://doi.org/10.1007/s13244-014-0342-4
31. Martin KW, McAlister WH, Shackelford GD. Acute renal infarction: diagnosis by doppler ultrasound. *Pediatr Radiol* 1988; **18**: 373–76. https://doi.org/10.1007/BF02388038
32. Suzer O, Shirkhoda A, Jafri SZ, Madrazo BL, Bis KG, Mastromatteo JF. CT features of renal infarction. *Eur J Radiol* 2002; **44**: 59–64. https://doi.org/10.1016/s0720-048x(01)00476-4
33. Paul GJ, Stephenson TF. The cortical rim sign in renal infarction. *Radiology* 1977; **122**(2): 338. https://doi.org/10.1148/122.2.338
34. Choo SW, Kim SH, Jeong YG, Shin YM, Kim JS, Han MC. MR imaging of segmental renal infarction: an experimental study. *Clin Radiol* 1997; **52**: 65–68. https://doi.org/10.1016/s0009-9260(97)80310-8
35. Heywood S, Tang V, Mare A, Tamhane R. Renal infarction with diffusion restriction changes on MRI. *Journal of Clinical Urology* 2018; **14**: 220–22. https://doi.org/10.1177/2051415818802967
36. Mertens PR, Duque-Reina D, Ittel TH, Keulers P, Sieberth HG. Contrast-enhanced computed tomography for demonstration of bilateral renal cortical necrosis. *Clin Investig* 1994; **72**: 499–501. https://doi.org/10.1007/BF00207477
37. Dyer RB, Chen MY, Zagoria RJ. Classic signs in uroradiology. *Radiographics* 2004; **24 Suppl 1**: S247-80. https://doi.org/10.1148/rg.24si045509
38. Chen F, Alexander L, Caserta M. Reverse rim sign on CEUS. *Abdom Radiol (NY)* 2020; **45**: 255–56. https://doi.org/10.1007/s00261-019-02273-z
39. Sweet DE, Feldman MK. *Multimodality vascular imaging: from head to toe*. Leesburg, VA: American Roentgen Ray Society; 2020, pp.75–85.
40. Erlich T, Kitrey ND. Renal trauma: the current best practice. *Ther Adv Urol* 2018; **10**: 295–303. https://doi.org/10.1177/1756287218785828
41. Shyu JY, Khurana B, Soto JA, Biffl WL, Camacho MA, et al, Expert Panel on Major Trauma Imaging. ACR appropriateness criteria® major blunt trauma. *J Am Coll Radiol* 2020; **17**: S160-74. https://doi.org/10.1016/j.jacr.2020.01.024
42. Kozar RA, Crandall M, Shanmuganathan K, Zarzaur BL, Coburn M, Cribari C, et al. Organ injury scaling 2018 update: spleen, liver, and kidney. *J Trauma Acute Care Surg* 2018; **85**: 1119–22. https://doi.org/10.1097/TA.0000000000002058
43. Brandes SB, McAninch JW. Reconstructive surgery for trauma of the upper urinary tract. *Urol Clin North Am* 1999; **26**: 183–99. https://doi.org/10.1016/s0094-0143(99)80016-0
44. Harris AC, Zwirewich CV, Lyburn ID, Torreggiani WC, Marchinkow LO. CT findings in blunt renal trauma. *Radiographics* 2001; **21 Spec No**: S201-14. https://doi.org/10.1148/radiographics.21.suppl_1.g01oc07s201